

Local structure of temperature and pH-sensitive colloidal microgels

Valentina Nigro, Roberta Angelini, Monica Bertoldo, Fabio Bruni, Valter Castelvetro, Maria Antonietta Ricci, Sarah Rogers, and Barbara Ruzicka

Citation: *The Journal of Chemical Physics* **143**, 114904 (2015); doi: 10.1063/1.4930885

View online: <http://dx.doi.org/10.1063/1.4930885>

View Table of Contents: <http://scitation.aip.org/content/aip/journal/jcp/143/11?ver=pdfcov>

Published by the [AIP Publishing](#)

Articles you may be interested in

[Stimulus-responsive colloidal sensors with fast holographic readout](#)

Appl. Phys. Lett. **107**, 051903 (2015); 10.1063/1.4928178

[Modeling the effects of pH and ionic strength on swelling of polyelectrolyte gels](#)

J. Chem. Phys. **142**, 114904 (2015); 10.1063/1.4914924

[Viscoelasticity of a colloidal gel during dynamical arrest: Evolution through the critical gel and comparison with a soft colloidal glass](#)

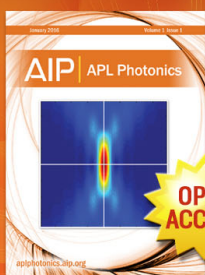
J. Rheol. **58**, 1557 (2014); 10.1122/1.4883675

[Ionic microgels as model systems for colloids with an ultrasoft electrosteric repulsion: Structure and thermodynamics](#)

J. Chem. Phys. **122**, 074903 (2005); 10.1063/1.1850451

[Small-angle neutron scattering study of structural changes in temperature sensitive microgel colloids](#)

J. Chem. Phys. **120**, 6197 (2004); 10.1063/1.1665752



Launching in 2016!

The future of applied photonics research is here

OPEN
ACCESS

AIP | APL
Photonics

Local structure of temperature and pH-sensitive colloidal microgels

Valentina Nigro,^{1,a)} Roberta Angelini,² Monica Bertoldo,³ Fabio Bruni,¹ Valter Castelvetro,⁴ Maria Antonietta Ricci,¹ Sarah Rogers,⁵ and Barbara Ruzicka²

¹*Dipartimento di Scienze, Sezione di Nanoscienze, Università degli Studi Roma Tre, Via della Vasca Navale 84, I-00146 Roma, Italy*

²*Istituto dei Sistemi Complessi del Consiglio Nazionale delle Ricerche (ISC-CNR) UOS Sapienza and Dipartimento di Fisica, Sapienza Università, Pz.le Aldo Moro 5, I-00185 Roma, Italy*

³*Istituto per i Processi Chimico-Fisici del Consiglio Nazionale delle Ricerche (IPCF-CNR), Area della Ricerca, Via G. Moruzzi 1, I-56124 Pisa, Italy*

⁴*Dipartimento di Chimica e Chimica Industriale, Università di Pisa, via G. Moruzzi 3, I-56126 Pisa, Italy*

⁵*ISIS-STFC, Rutherford Appleton Laboratory, Chilton, Oxon OX11 0QX, United Kingdom*

(Received 14 May 2015; accepted 1 September 2015; published online 18 September 2015)

The temperature dependence of the local intra-particle structure of colloidal microgel particles, composed of interpenetrated polymer networks, has been investigated by small-angle neutron scattering at different pH and concentrations, in the range (299 ÷ 315) K, where a volume phase transition from a swollen to a shrunken state takes place. Data are well described by a theoretical model that takes into account the presence of both interpenetrated polymer networks and cross-linkers. Two different behaviors are found across the volume phase transition. At neutral pH and $T \approx 307$ K, a sharp change of the local structure from a water rich open inhomogeneous interpenetrated polymer network to a homogeneous porous solid-like structure after expelling water is observed. Differently, at acidic pH, the local structure changes almost continuously. These findings demonstrate that a fine control of the pH of the system allows to tune the sharpness of the volume-phase transition. © 2015 AIP Publishing LLC. [<http://dx.doi.org/10.1063/1.4930885>]

I. INTRODUCTION

Colloidal microgels are aqueous dispersions of nano- or micro-metre sized hydrogel particles with high sensitivity to external stimuli such as pH, temperature, electric field, ionic strength, solvent, external stress, or light. These are therefore particularly interesting smart materials^{1–4} and have attracted great attention due to their impact on both industry and fundamental science. Indeed, colloidal microgels have applications in agriculture, construction, cosmetics and pharmaceuticals industries, in artificial organs, and tissue engineering.^{2,3,5–8} On the other hand, the interaction potential between microgel particles can be modulated through parameters usually not so relevant in ordinary colloidal systems. Indeed, it can be easily controlled⁹ not only by tuning the common external parameters, such as packing fraction, waiting time (ageing), and ionic strength, but also by varying temperature and pH, making these materials new model systems for understanding the physics of dynamical arrest, compared to atomic and molecular glasses.^{10–13}

The characterization of several colloidal systems through experimental techniques has shown the existence of different arrested states (such as gels^{14–16} and glasses^{17,18}) and unusual glass-glass transitions.^{19–21} In particular, soft colloidal systems, such as responsive microgels, lead to unusual transition between different arrested states as theoretically predicted^{22–24} and recently experimentally observed.^{25,26}

One of the most studied responsive microgels is based on the poly(N-isopropylacrylamide), also known as PNIPAM, a thermo-sensitive polymer, synthesized in colloidal form for the first time in 1986 by Pelton and Chibante.²⁷ Since then, both experiments and theoretical works have provided a clear picture of preparation, characterization, and applications.^{1–4,25,28} It is now clear that PNIPAM microgels responsiveness is strongly dependent on the thermo-sensitivity of PNIPAM that in water presents a lower critical solution temperature at about 305 K. At room temperature indeed, PNIPAM microgels are in a swollen state due to the polymer hydrophilicity, which leads to dominant polymer-solvent interactions and to the retention of a great amount of water. By increasing temperature above 307–309 K, the polymer becomes hydrophobic and in this case, the polymer-polymer interactions become dominant. Due to the polymer chains collapse, water is completely expelled, giving rise to a volume phase transition (VPT) towards a shrunken state. Similar characteristic VPT behavior, due to the temperature sensitivity of PNIPAM polymer, can be expected in any PNIPAM based microgel.²⁹ In the last years, the phase diagram^{25,30,31} and other important details on the structural and dynamical properties of PNIPAM microgels near the volume phase transition have been obtained.^{32–34} Moreover, it has been recently shown that the microgel swelling/deswelling behavior can be strongly affected by concentration,^{25,35} by solvents,³⁶ and by the synthesis procedure,³⁷ such as growing number of cross-linking points,^{38,39} different reaction pH conditions,⁴⁰ or by introducing additives into the PNIPAM network.^{41,42}

^{a)}Electronic mail: nigro@fis.uniroma3.it

In this context, PNIPAM microgels containing another species as co-monomer or interpenetrated polymer are deemed to be even more interesting systems, since a deeper control of the phase behavior in response to different environmental conditions is possible, yet preserving the main properties of the constituent polymers. In particular, addition of acrylic acid (AAc) polymer to PNIPAM microgel can provide an additional pH-sensitivity to the system, obtaining a thermo- and pH-sensitive material with a more complex phase behavior and a more attractive smart response to the external stimuli.³⁷ Indeed, a volume phase transition with temperature is observed also in these systems, although their swelling capability is reduced with increasing the AAc concentration.^{43,44} The volume phase transition of these microgels is strongly dependent on the effective charge density controlled by the content of AAc monomer,^{43,44} on the pH of the suspension,^{45–48} and on the salt concentration.^{45,49} In this framework, the synthesis procedure plays an important role and the chosen route for the incorporation of AAc into PNIPAM gives rise to systems with interesting differences in their behavior.³⁷ Indeed, the microgel obtained by random copolymerization (NIPAM-co-AAc)^{45,46,48–53} is characterized by particles composed of a single network of both monomers, with properties dependent on the monomer ratio.⁴⁵ Conversely, the microgel obtained by polymer interpenetration, usually referred to as PNIPAM-PAAc Interpenetrated Polymer Network (IPN) microgel,^{43,47,54–56} is composed of microgel particles made of two interpenetrated homopolymeric networks of PNIPAM and PAAc, each preserving its independent responsiveness to the external stimuli.⁵⁴ In IPN microgels, the mutual interference between the temperature-responsive and pH-responsive polymers is largely reduced, thus preserving the temperature dependence of the VPT of pure PNIPAM microgel (with the transition close to the physiological temperature) in a microgel (IPN) that is more suitable for applications in controlled drug release and sensors,^{5,57} due to the additional pH sensitivity.

A few investigations through Dynamic Light Scattering (DLS), rheology and microscopic techniques have confirmed the existence of the VPT also in IPN microgels^{47,54–56,58} and proposed a preliminary temperature-concentration phase diagram.⁴³ Nevertheless, the dependence on pH, ionic strength, and cross-link density have been left unexplored up to now, and only recently some studies⁵⁹ have taken into account the role played by the pH of the solution in the swelling behavior. Indeed, it has been shown that the swelling capability is widely reduced when the acrylic acid is introduced, due to the insolubility of PAAc in water at acidic conditions. Apparently, it can be completely restored by increasing the pH of the solution, due to the induced deprotonation of the carboxylic groups of the acrylic acid. In addition, an interesting dependence on concentration of the swelling/shrinking transition has been observed at both acidic and neutral pH conditions.

Although the macroscopic swelling behavior of the PNIPAM/PAAc IPN microgel particles has been largely clarified, the response of their inner local structure to changes of the external parameters is still an open issue. Small-Angle Neutron Scattering (SANS) is a relevant technique for investigations

of the spatial inhomogeneities in the length scale from a few tens of angstroms to thousands of angstroms, thanks to the accessibility of low values of the wavevectors, Q . Indeed, previous SANS studies on PNIPAM microgels have shown the existence of intermediate states between the fully swollen and the completely shrunken phases.⁶⁰ In this work, we present a SANS study performed on IPN microgel particles of PNIPAM and PAAc dispersed in water, by changing the temperature across the VPT, at two pH values and three concentrations, in order to evaluate the response of the intra-particle structure to changes of these external parameters.

II. EXPERIMENTAL

A. Materials

1. Materials

Both *N*-isopropylacrylamide (NIPAM) from Sigma-Aldrich and *N,N'*-methylene-bis-acrylamide (BIS) from Eastman Kodak were purified from hexane and methanol, respectively, by recrystallization, dried under reduced pressure (0.01 mm Hg) at room temperature, and stored at 253 K until used. AAc from Sigma-Aldrich was purified by distillation (40 mm Hg, 337 K) under nitrogen atmosphere in the presence of hydroquinone and stored at 253 K until used. Sodium dodecyl sulphate (SDS), 98% purity, potassium persulfate (KPS), 98% purity, ammonium persulfate, 98% purity, *N,N,N',N'*-tetramethylethylenediamine (TEMED), 99% purity, and ethylenediaminetetraacetic acid (EDTA), NaHCO₃, were all purchased from Sigma-Aldrich and used as received. Ultrapure water (resistivity: 18.2 M Ω /cm at 298 K) was obtained with Sarium[®] pro Ultrapure Water purification Systems, Sartorius Stedim from demineralized water, and D₂O (99.9 atom%) from Sigma-Aldrich. All other solvents were RP grade (Carlo Erba) and were used as received. A dialysis tubing cellulose membrane, HCWO 14 000 Da, from Sigma-Aldrich, was cleaned before use by washing in running distilled water for 3 h, treating at 343 K for 10 min into a solution containing a 3.0% weight concentration of NaHCO₃ and 0.4% of EDTA, and rinsing in distilled water at 343 K for 10 min and finally in fresh distilled water at room temperature for 2 h.

2. Synthesis of IPN microparticles

The IPN microgel was synthesized by a sequential free radical polymerization method. In the first step, PNIPAM micro-particles were synthesized by precipitation polymerization. In the second step, acrylic acid was polymerized into the preformed PNIPAM network.⁴³ (4.0850 \pm 0.0001) g of NIPAM, (0.0695 \pm 0.0001) g of BIS, and (0.5990 \pm 0.0001) g of SDS were solubilized in 300 ml of ultrapure water and transferred into a 500 ml five-necked jacketed reactor equipped with condenser and mechanical stirrer. The solution was deoxygenated by purging with nitrogen for 30 min and then heated at (273.0 \pm 0.3) K. (0.1780 \pm 0.0001) g of KPS (dissolved in 5 ml of deoxygenated water) was added to initiate the polymerization and the reaction was allowed to proceed for 4 h. The resultant PNIPAM microgel was purified by dialysis

against distilled water with frequent water change for 2 weeks. The final weight concentration and diameter of PNIPAM micro-particles were 1.02% and 80 nm (at 298 K) as determined by gravimetric and DLS measurements, respectively. (65.45 ± 0.01) g of the recovered PNIPAM dispersion and (0.50 ± 0.01) g of BIS were mixed and diluted with ultrapure water up to a volume of 320 ml. The mixture was transferred into a 500 ml five-necked jacketed reactor kept at (295 ± 1) K by circulating water and deoxygenated by purging with nitrogen for 1 h. 2.3 ml of AAc and (0.2016 ± 0.0001) g of TEMED were added and the polymerization was started with (0.2078 ± 0.0001) g of ammonium persulfate (dissolved in 5 ml of deoxygenated water). The reaction was allowed to proceed for 65 min and then stopped by exposing to air. The obtained IPN microgel was purified by dialysis against distilled water with frequent water change for 2 weeks, and then lyophilized to constant weight. The PAAc second network amount in the IPN was 31.5% by gravimetric analysis and the acrylic acid monomer units content was 22% by acid/base titration. The remaining 9.5% is being ascribed to BIS.⁶¹

3. Sample preparation

40 mg of lyophilized IPN was dispersed in 10 g of D₂O by magnetic stirring for 1 day. The sample was lyophilized and redispersed again in D₂O to a final weight concentration of 0.310%. Samples at different concentrations were obtained by dilution with D₂O.

4. Characterization

The poly(acrylic acid) content in 10 g of IPN dispersion was determined by addition of 11 ml of 0.1M NaOH, followed by potentiometric back titration with 0.1M hydrochloric acid. The concentration of the dispersion was determined from the weight of the residuum after water removal by lyophilization, corrected for the moisture residual amount obtained by thermogravimetric analysis (TGA). This was accomplished with a SII Nano-Technology EXTAR TG/DTA7220 thermal analyzer at 275 K/min in nitrogen atmosphere (200 ml/min). 5 mg of sample in an alumina pan was analyzed in the (313–473) K temperature range and the weight loss was assumed as moisture content.

Moreover, DLS measurements performed on aqueous suspensions of IPN microgels⁵⁹ show a cross-over at around 305 K–307 K from a completely swollen state, with particle diameter of about 4000–5000 Å, to a completely shrunken one, with diameter of about 2000–3000 Å. In Fig. 1, the temperature behavior of the normalized hydrodynamic radius of aqueous suspensions of IPN microgels at pH 5 and 7 and at weight concentration $C_w = 0.10\%$ compared to PNIPAM microgels is shown.

B. SANS experiment and data analysis

SANS measurements have been performed on the SANS2d instrument at the 10 Hz pulsed neutron source ISIS-TS2.⁶² The scattering geometry of this instrument has been set up to use a Q-range from 0.004 to 0.7 Å⁻¹, cor-

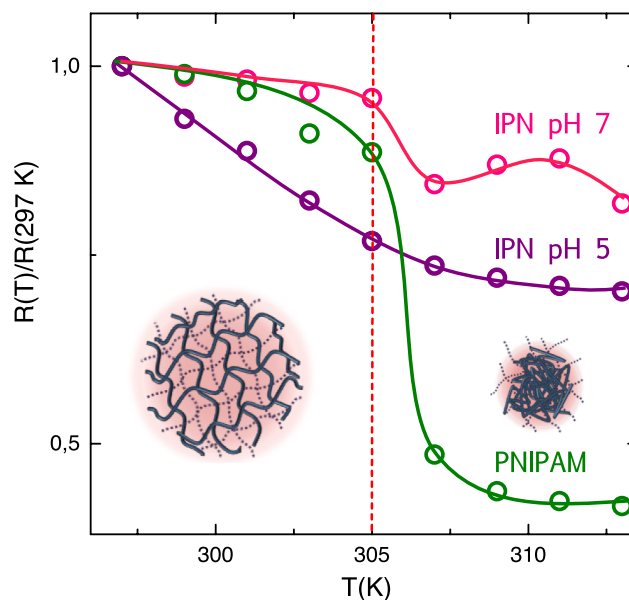


FIG. 1. Temperature behavior of the normalized hydrodynamic radius obtained from DLS measurements, for aqueous suspensions of IPN microgels at pH 5 and 7 and PNIPAM microgels, both at the weight concentration $C_w = 0.1\%$. Solid lines are guides to eyes.

responding to length scale from ~10 to ~1500 Å. Since the average diameter of the microgel particles is in the range 2000–5000 Å, our measurements allow to look inside them and to explore changes of their local structure during the cross-over from the fully swollen to the completely shrunken phase, as similarly observed on PNIPAM microgel suspensions.^{60,63,64} Measurements have been performed at five temperatures in the range $T = (299 \div 315)$ K, at pH 5 and 7 and at weight concentrations $C_w = 0.084\%$, 0.170%, and 0.310%, where all samples are liquid far from the gel/glass transition.

The SANS coherent differential cross-section $I(Q)$ is

$$I(Q) = (\Delta\rho)^2 n V_{polymer}^2 P(Q) S(Q), \quad (1)$$

where $Q = 4\pi \sin(\theta/2)/\lambda$ is the exchanged wave vector, $\Delta\rho$ is the contrast factor between the polymer and the surrounding solvent, n is the number density of the particles, $V_{polymer}$ is the volume of polymer within the particle, $P(Q)$ is the form factor accounting for interference of neutrons scattered by polymer segments within the same particle, and $S(Q)$ is the static structure factor which accounts for the interference of neutrons scattered by different particles. In dilute suspensions, as those investigated here, the static structure factor can be assumed equal to 1 and the Q dependence of the scattered intensity reflects only the internal structure of the particles. Thus, the problem is reduced to model the form factor $P(Q)$. In addition to the coherent contribution, SANS data show an incoherent, flat background, depending on the atomic composition of the sample. This contribution has no useful structural information and is usually assumed to be the same as a reference sample having the same transmission as the measured one, without structures at low Q. In the present experiment, the measured SANS signal from a pure D₂O sample has been subtracted from the raw data to get the $I(Q)$ defined in Eq. (1). In the case of colloidal suspensions of microgel particles, finding a suitable scattering function may be complicated, due to the complexity

of the synthesis process. Indeed, when a cross-linker generating the network is introduced, the polymer chains become connected one to each other determining nonuniformity in the distribution and concentration of the polymer chains and leading to constraints to their relative arrangements. It has been found^{60,65} that similar network systems can be modeled through a deformable lattice model of blobs and, in particular, according to Shibayama *et al.*,^{60,64,66} with the expression,

$$I(Q) = \frac{I_L(0)}{\{1 + [(D+1)/3]\xi^2 Q^2\}^{D/2}} + I_G(0)\exp(-R_g^2 Q^2/3), \quad (2)$$

where $I_L(0)$ and $I_G(0)$ are scale factors dependent on the polymer-solvent contrast and on the volume fraction of the microgel, ξ is the correlation length related to the size of the polymer network mesh and D is the Porod exponent, giving an estimate of the roughness of the interfaces between different domains of inhomogeneities. In the limit of non-interacting domains, the dense regions can be assumed to be randomly distributed within the network. Hence, the spatial distribution of such regions is assumed to be a Gaussian, with standard deviation R_g . Due to the equivalence with the Guinier function, R_g can be interpreted as the mean size of the polymer-rich or -poor domains, that is, the static inhomogeneities introduced into the network by the chemical cross-links.⁶⁶ On the other hand, the Lorentzian term describes the fluctuations of the chains density and the interchains interactions which account for the thermodynamics of the swollen network.

This model has been successfully used to reproduce the temperature and concentration dependence of the spatial inhomogeneities of PNIPAM microgel particles undergoing a continuous volume-phase transition⁶⁰ at a macroscopic level. Here the same approach has been adopted to describe the local structure behavior of our IPN microgel particles, at each temperature, pH, and concentration.

In Fig. 2, the fitted spectra for two samples at fixed weight concentration $C_w = 0.084\%$ and neutral pH are reported, as an

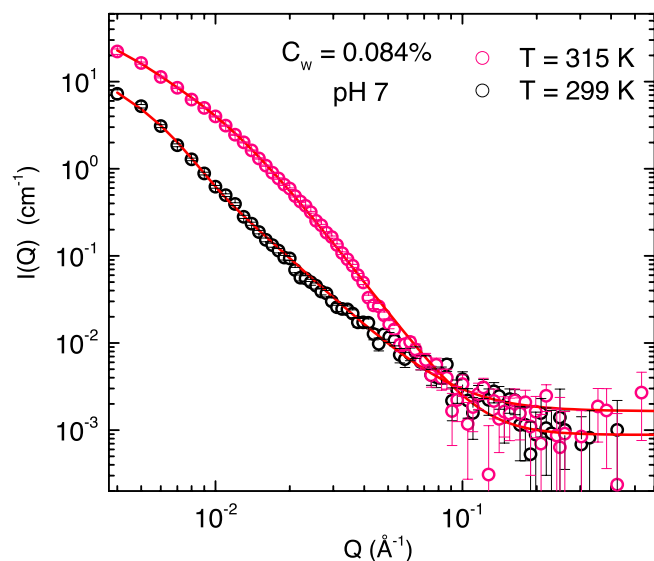


FIG. 2. Differential cross section of a $C_w = 0.084\%$ sample at pH 7 for two temperatures, $T = 299$ K (black circles) and $T = 315$ K (red circles), respectively, below and above the VPT. Solid lines are fits according to Eq. (2).

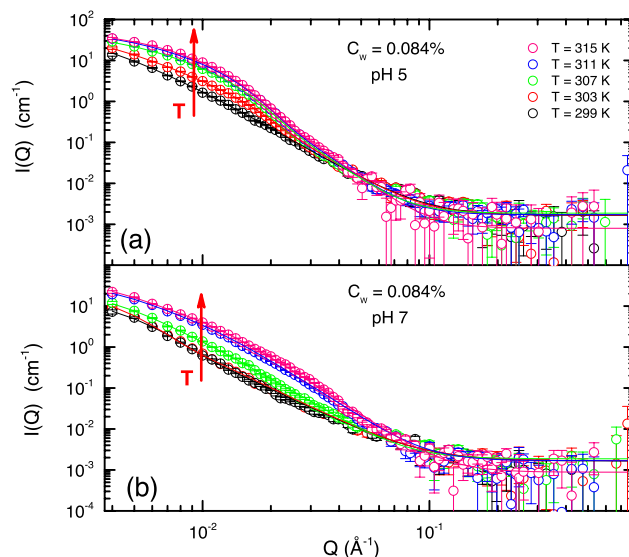


FIG. 3. Differential cross section of $C_w = 0.084\%$ samples at (a) pH 5 and (b) pH 7 in the temperature range $T = (299 \div 315)$ K: experimental data are reported as circles and their fits as solid lines. The arrows indicate increasing temperature.

example, at two different temperatures (below and above the VPT). As shown, the model accurately fits our data, suggesting that it can be used to properly analyze the local structure of a colloidal suspension of microgels, also in the presence of interpenetrated polymer networks. The fits of all other data over all the Q range as reported in Figs. 3 and 4 are of the same high quality of those discussed above (Fig. 2), with structureless residuals and normalized χ^2 of the order of 1.

III. RESULTS AND DISCUSSION

In Fig. 3, the temperature behavior of the spectra collected at $C_w = 0.084\%$ and at pH 5 and 7 is reported, as an example.

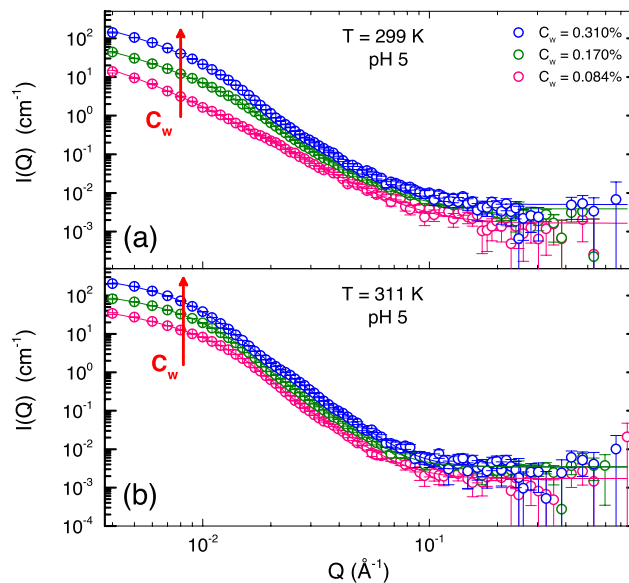


FIG. 4. Differential cross section at pH 5 and two values of temperature below and above the VPT, namely, (a) $T = 299$ K and (b) $T = 311$ K, for three different concentrations $C_w = 0.084\%$, 0.170% , and 0.310% . Experimental data are reported as circles and their fits as solid lines. The arrows indicate increasing concentration.

As the temperature or the pH varies, the spectral shape clearly changes at both low and intermediate Q values, suggesting a significant response of the microgel particle structure at different length scales. Indeed, the excess static scattering at low Q values is associated to densely crosslinked regions, while the scattering at higher Q is dominated by the contribution of the surrounding swollen matrix with a solution-like behavior. With increasing temperature, an increase of the intensity at very low Q , $I_L(0) + I_G(0)$, and of the slope, D , at higher Q values is observed. The increase of the neutron contrast/scattering intensity is due to the collapse of the polymer chains above the VPT, which leads to a more homogeneous local structure within the microgel particles, whilst the increase of the Porod exponent D is due to the decrease of roughness of the domain interfaces. However, the role played by PAAc in modulating the response of the local structure determines interesting differences at either acidic or neutral conditions. Samples at pH 5 exhibit a continuous variation of the low Q intensity, suggesting a smooth macroscopic transition from a swollen to a shrunken state at temperatures around 305 K. On the contrary, the transition becomes more evident at neutral pH. This behavior is related to the solvation in water of the PAAc chains at pH values above 5.5, due to its deprotonation, with a complete regain of the swelling capability of the system. Moreover, the changes of D observed at higher Q values are more pronounced at pH 7, reflecting a macroscopic transition from states characterized by different structural features.

Finally, we notice a concentration dependence of the microgel particles structural response both above and below the VPT (see Fig. 4). Indeed, both the low Q intensity and the slope, D , of the differential cross section at high Q increase with concentration at fixed pH and temperature. The change with the concentration is probably tuned by the pH, as we will comment later.

The local intra-particle structural response to external parameters has been rationalized by looking at the behavior of the correlation length ξ and the Porod exponent D , obtained from the Lorentzian contribution of Eq. (2). Their behavior, reported in Fig. 5 as a function of temperature at both acidic and

neutral pH, for three different concentrations, highlights the existence of a transition from an inhomogeneous to a porous solid-like structure across the VPT.

At pH 5, the correlation length ξ decreases with temperature, showing a transition to a plateau value above 305 K (Fig. 5(a)). A similar, although less dramatic, change from a clear temperature dependence to an almost constant value is observed for the Porod exponent D (Fig. 5(b)). Moreover, in this case, a spread of the Porod coefficient is visible already at low temperatures and masks the transition, in particular at the highest concentrations. Therefore, a sharp transition at the VPT is not evidenced. Instead, at pH 7, although in this case, a plateau is not reached in the investigated temperature range, a sharper transition is identified at $T \approx 305$ K in the behavior of both the correlation length (Fig. 5(c)) and the Porod exponent (Fig. 5(d)).

By increasing the pH above 5.5, the deprotonation of the PAAc chains results in their effective hydration and the two networks are independent. Therefore, at neutral pH, above the VPT, the PNIPAM network collapses, while the PAAc chains do not. Below the VPT, where the polymer coils are completely swollen, the microgel particles have a rough domain surface ($D \approx 3$); on the contrary, above the VPT, they switch to a homogeneous solid-like structure, with smooth interfaces between different domains ($D \approx 4$). Additionally, a different behavior with concentration of both the correlation length and the Porod exponent across the transition can be noticed, at the two investigated pH values. At acidic pH, both parameters for the less concentrated sample show the most intense variation with increasing temperature. On the contrary, at pH 7, this trend is reversed: the most concentrated sample shows the largest variation of ξ and D across the transition and this gap decreases with concentration. This behavior suggests that the role played by the concentration is not trivial and may confirm the features of the swelling behavior observed through DLS measurements at larger length scales.⁵⁹

From the Gaussian contribution of Eq. (2), one can obtain information about the mean size R_g of those regions of the lattice with restricted dynamics and higher polymer density, due to the presence of cross-links. The behavior of the parameter R_g is shown in Fig. 6 as a function of temperature and concentration at both pH 5 and 7.

The average size of the polymer-rich domains (R_g) increases with temperature, suggesting a transition from an inhomogeneous structure in the swollen state to a porous solid-like structure, where a unique larger sized cluster is formed, due to the shrinking of the polymer chains. R_g increases with temperature at both acidic and neutral pH conditions; nevertheless, at pH 7, an evident discontinuity shows up at $T \approx 305$ K, around the expected VPT, thus confirming the regained swelling at neutral pH. On the contrary, at pH 5, the differences between polymer-rich and polymer-poor domains are less marked and the elastic response of the system to temperature changes is limited by the presence of the PAAc chains. Indeed, at pH 5, the PAAc chains are not effectively solvated by water and the formation of H-bonds between PAAc and PNIPAM is favored,⁶⁷ as shown in the cartoon of Fig. 7(a), thus introducing spatial constraints which limit the PNIPAM network swelling. At neutral pH instead, both compounds are solvated by water

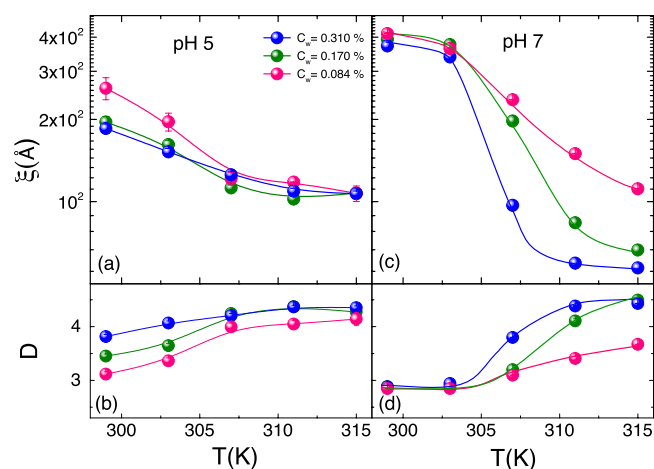


FIG. 5. Correlation length, ξ , and Porod exponent, D , as a function of temperature for three fixed concentrations $C_w = 0.084\%$, 0.170% , and 0.310% and two pH values, namely, pH 5, panels (a) and (b), and pH 7, panels (c) and (d). Full lines are guides to eyes.

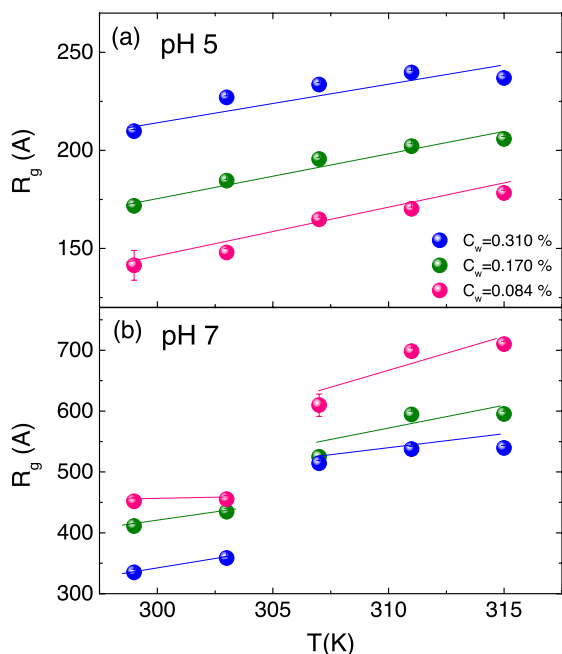


FIG. 6. Gyration radius of the static inhomogeneities as a function of temperature and for three fixed concentrations $C_w = 0.084\%$, 0.170% , and 0.310% at acidic (a) and neutral (b) pH condition. Full lines are guides to eyes.

that mediates their interaction, giving rise to a lower number of interchain H-bonds (Fig. 7(a)). Therefore, the H-bonds, depending on the pH, highly affect the swelling behaviour of the system. Moreover, H-bonding between the PNIPAM and PAAc chains determines additional inhomogeneities in the structure of microgel particles with smaller size compared to the high density regions formed by crosslinking. As a consequence, R_g is the average size between two different inhomogeneity domains and at acidic pH, it results smaller compared to neutral conditions (where H-bonds do not form).

We notice also that the concentration dependence is reversed at neutral and acidic pH: at neutral pH, the most concentrated sample shows the lowest value of R_g , suggesting that the spatial distribution of polymer-rich (or poor) domains becomes narrower as the concentration increases. This behavior seems to confirm the concentration dependence observed by DLS measurements and deserves deeper investigation.

These results return a simple model of the internal structure of the microgel particles across the VPT, shown in the cartoon of Fig. 7(b). The IPN microgels internal structure undergoes a transition from an inhomogeneous interpenetrated network (where dense regions of size R_g are separated by a lower density network of size ξ) to a porous solid-like structure, where the typical nanometric structure of the tridimensional network is lost, as a consequence of the macroscopic swelling/shrinking transition. When the polymer chains are completely swollen, the open network can accommodate a large amount of water, resulting in an inhomogeneous intraparticle structure of high contrast between polymer-rich and -poor regions. With increasing temperature, the collapse of the polymer chains leads to the expulsion of water molecules along with a shrinking of the microgel particles whose local structure becomes more homogeneous and characterized by correlation

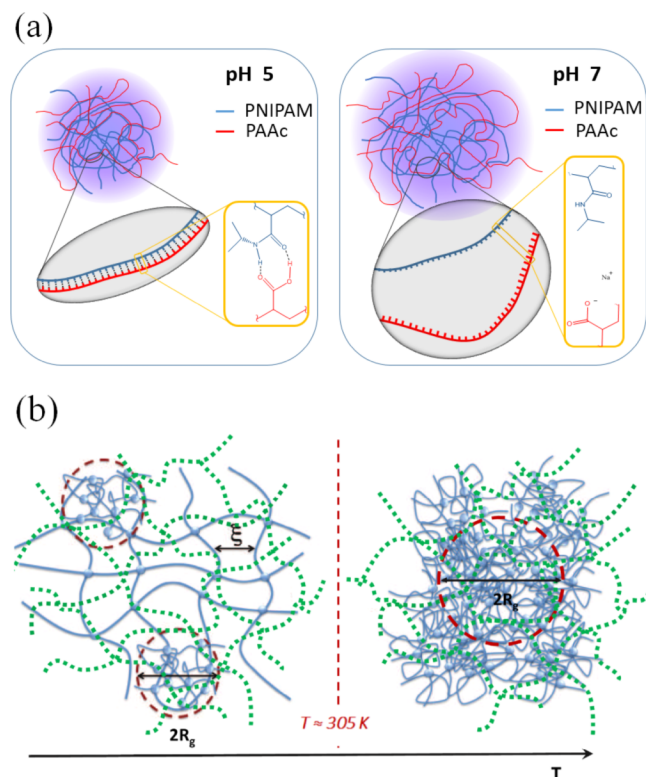


FIG. 7. (a) Cartoon of the interaction between the PAAc chains (red) and the PNIPAM chains (blue) at acidic conditions (left panel) and at neutral pH (right panel). Hydrogen bonds are formed when the pH of the solution is lower than the critical value of solubility of PAAc and determine additional constraints to the interpenetrated network. (b) Cartoon of the local structure inside the IPN microgel particle below (left side) and above (right side) the VPT. The solid and dashed lines represent the two interpenetrating networks with average mesh size ξ . The dashed red circles in the left side panel (swollen state) evidence the regions of quenched inhomogeneities of average size (radius) R_g , due to the presence of cross-links. With increasing temperature, the collapse of the polymer networks induces a transition from an inhomogeneous structure to a porous solid-like structure (right side panel).

domains with smoother interfaces. As a consequence, the short correlation length, ξ , decreases when the microgel particles collapse. Instead, the Porod exponent, D , associated to the roughness of the correlation domains interfaces, increases, since their surface becomes smoother as the degree of inhomogeneity within the polymer network decreases. Furthermore, the collapse of the polymer chains leads to the loss of individuality of the frozen blobs within the microgel particle which can be interpreted as an infinite cluster of cross-link points leading to the R_g increasing.

IV. CONCLUSIONS

The intra-particle structure of colloidal suspensions of IPN microgels composed by interpenetrated network of PNIPAM and PAAc has been characterized by SANS. By increasing temperature, the IPN microgels undergo a volume-phase transition from a water-rich open inhomogeneous interpenetrated polymer network to a homogeneous porous solid-like structure, accompanied by water release. Correspondingly, a clear change of the local structure of the microgel particles is observed. Below the VPT, when the polymer network forming the microgel particles is swollen, its local structure is

characterized by regions with restricted dynamics due to the elastic constraints brought about by the presence of cross-linking sites. The typical size of these regions, R_g , between 150 and 500 Å, depends on pH and weight concentration and is related to the different elastic responses of the sample at acidic and neutral pH conditions and at different concentrations.

Below the VPT, these domains of static inhomogeneities are well separated and connected throughout the polymer networks, with average mesh size of the order of a few hundreds of Å. Moreover, due to the expansion of the hydrophilic polymer in water, the interface between adjacent domains is rough. The inhomogeneities within the structure are best evident at neutral pH when the PNIPAM network regains its swelling capability, while at acidic pH, the topological constraints introduced by the H-bonds between the PAAc and the PNIPAM chains limit the swelling of the network, so that differences between polymer-poor or -rich domains are less appreciable.

Above the VPT, when water is expelled from the particles, a transition to a more homogeneous local structure is found as a consequence of the shrinking of the network. This structure is characterized by shorter mesh size and larger domains of static inhomogeneities, separated by smoother interfaces. In addition, an interesting concentration dependence with an inversion of trend at neutral pH with respect to the acidic conditions has been observed. Indeed at pH 5 the less concentrated sample exhibits the more intense response to temperature changes, while at pH 7, the opposite trend is observed. These findings confirm our DLS preliminary results,⁵⁹ showing that besides the expected behavior with pH and temperature, a concentration dependence of the swelling at higher length scale is found.

In summary, IPN microgel particles show a structural transition, corresponding to the VPT at larger length scales, at physiological temperature, with a sharpness that can be tuned according to the application needs by the pH of the environment. These properties highlight an interesting balance between polymer-polymer and polymer-water interactions that is expected to drive the dynamical arrest at higher weight concentrations. It is likely indeed that different arrested states can be found at different pH values, thus offering a new ground for fundamental studies of the gel/glass transition. Moreover, the tunability of the sharpness of the VPT and water release by the pH of the environment makes this material very promising for applications as drug delivery.

ACKNOWLEDGMENTS

This work has been performed within the Agreement No. 01/9001 between Science and Technology Facilities Council (STFC) and Consiglio Nazionale delle Ricerche (CNR), concerning collaboration in scientific research at the Spallation Neutron Source ISIS and with partial financial support of CNR. R.A. acknowledges support from MIUR-PRIN (2012J8X57P).

¹B. R. Saunders and B. Vincent, "Microgels particles as model colloids: Theory, properties and applications," *Adv. Colloid Interface Sci.* **80**, 1–25 (1999).

²R. H. Pelton, "Temperature-sensitive aqueous microgels," *Adv. Colloid Interface Sci.* **85**, 1–33 (2000).

³M. Das, H. Zhang, and E. Kumacheva, "MICROGELS: Old materials with new applications," *Annu. Rev. Mater. Res.* **36**, 117–142 (2006).

⁴M. Karg and T. Hellweg, "New "smart" poly(NIPAM) microgels and nanoparticle microgel hybrids: Properties and advances in characterisation," *Curr. Opin. Colloid Interface Sci.* **14**, 438–450 (2009).

⁵J. S. Park, H. N. Yang, D. G. Woo, S. Y. Jeon, and K. H. Park, "Poly(N-isopropylacrylamide-co-acrylic acid) nanogels for tracing and delivering genes to human mesenchymal stem cells," *Biomaterials* **34**, 8819–8834 (2013).

⁶P. Schexnailder and G. Schmidt, "Nanocomposite polymer hydrogels," *Colloid Polym. Sci.* **287**, 1–11 (2009).

⁷N. M. B. Smeets and T. Hoare, "Designing responsive microgels for drug delivery applications," *J. Polym. Sci., Part A: Polym. Chem.* **51**, 3027–3043 (2013).

⁸S. Su, A. M. Monsur, C. D. M. Filipe, Y. Li, and R. H. Pelton, "Microgel-based inks for paper-supported biosensing applications," *Biomacromolecules* **9**, 935–9419 (2008).

⁹C. N. Likos, "Effective interactions in soft condensed matter physics," *Phys. Rep.* **348**, 267–439 (2001).

¹⁰F. Sciortino and P. Tartaglia, "Glassy colloidal systems," *Adv. Phys.* **54**, 471–524 (2005).

¹¹V. Trappe and P. Sandkühler, "Colloidal gels - low-density disordered solid-like states," *Curr. Opin. Colloid Interface Sci.* **8**, 494 (2004).

¹²W. C. K. Poon, "Phase separation, aggregation and gelation in colloid polymer mixtures and related systems," *Curr. Opin. Colloid Interface Sci.* **3**, 593 (1998).

¹³E. Zaccarelli, "Gelation as arrested phase separation in short-ranged attractive colloid-polymer mixture," *J. Phys.: Condens. Matter* **20**, 494242 (2008).

¹⁴P. J. Lu, E. Zaccarelli, F. Ciulla, A. B. Schofield, F. Sciortino, and D. A. Weitz, "Gelation of particle with short range attraction," *Nature* **453**, 499–503 (2008).

¹⁵C. P. Royall, S. R. Williams, T. Ohtsuka, and H. Tanaka, "Direct observation of a local structural mechanism for dynamical arrest," *Nat. Mater.* **7**, 556–561 (2008).

¹⁶B. Ruzicka, E. Zaccarelli, L. Zulian, R. Angelini, M. Sztucki, A. Moussaïd, T. Narayanan, and F. Sciortino, "Observation of empty liquids and equilibrium gels in a colloidal clay," *Nat. Mater.* **10**, 56 (2011).

¹⁷P. N. Pusey and W. van Megen, "Phase behaviour of concentrated suspensions of nearly hard colloidal spheres," *Nature* **320**, 340 (1986).

¹⁸A. Imhof and J. K. G. Dhont, "Experimental phase diagram of a binary colloidal hard-sphere mixture with a large size ratio," *Phys. Rev. Lett.* **75**, 1662–1665 (1995).

¹⁹K. N. Pham, A. M. Puertas, J. Bergenholtz, S. U. Egelhaaf, A. Moussaïd, P. N. Pusey, A. B. Schofield, M. E. Cates, M. Fuchs, and W. C. K. Poon, "Multiple glassy states in a simple model system," *Science* **296**, 104 (2002).

²⁰T. Eckert and E. Bartsch, "Re-entrant glass transition in a colloid-polymer mixture with depletion attractions," *Phys. Rev. Lett.* **89**, 125701 (2002).

²¹R. Angelini, E. Zaccarelli, F. A. de Melo Marques, M. Sztucki, A. Fluerau, G. Ruocco, and B. Ruzicka, "Glass-glass transition during aging of a colloidal clay," *Nat. Commun.* **5**, 4049 (2014).

²²C. N. Likos, N. Hoffmann, H. Lowen, and A. A. Louis, "Exotic fluids and crystals of soft polymeric colloids," *J. Phys.: Condens. Matter* **14**, 7681–7698 (2002).

²³P. E. Ramírez-González and M. Medina-Noyola, "Glass transition in soft-sphere dispersions," *J. Phys.: Condens. Matter* **21**, 075101 (2009).

²⁴D. M. Heyes, S. M. Clarke, and A. C. Brank, "Elasticity of compressed microgel suspensions," *J. Chem. Phys.* **131**, 204506 (2009).

²⁵H. Wang, X. Wu, Z. Zhu, C. S. Liu, and Z. Zhang, "Revisit to phase diagram of poly(N-isopropylacrylamide) microgel suspensions by mechanical spectroscopy," *J. Chem. Phys.* **140**, 024908 (2014).

²⁶J. Mattsson, H. M. Wyss, A. Fernandez-Nieves, K. Miyazaki, Z. Hu, D. Reichman, and D. A. Weitz, "Soft colloids make strong glasses," *Nature* **462**, 83–86 (2009).

²⁷R. H. Pelton and P. Chibante, "Preparation of aqueous lattices with N-isopropylacrylamide," *Colloids Surf.* **20**, 247–256 (1986).

²⁸Y. Lu and M. Ballauff, "Thermosensitive core-shell microgels: From colloidal model systems to nanoreactors," *Prog. Polym. Sci.* **36**, 767–792 (2011).

²⁹J. Wu, G. Huang, and Z. Hu, "Interparticle potential and the phase behavior of temperature-sensitive microgel dispersions," *Macromolecules* **36**, 440–448 (2003).

³⁰J. Wu, B. Zhou, and Z. Hu, "Phase behavior of thermally responsive microgel colloids," *Phys. Rev. Lett.* **90**, 048304 (2003).

³¹D. Paloli, P. S. Mohanty, J. J. Crassous, E. Zaccarelli, and P. Schurtenberger, "Fluid–solid transitions in soft-repulsive colloids," *Soft Matter* (2012).

- ³²J. Gao and Z. Hu, "Optical properties of N-isopropylacrylamide microgel spheres in water," *Langmuir* **18**, 1360–1367 (2002).
- ³³S. Tang and Z. Hu, "Crystallization kinetics of thermosensitive colloids probed by transmission spectroscopy," *Langmuir* **20**, 8858–8864 (2004).
- ³⁴P. S. Mohanty, D. Paloli, J. J. Crassous, E. Zaccarelli, and P. Schurtenberger, "Effective interactions between soft-repulsive colloids: Experiments, theory and simulations," *J. Chem. Phys.* **140**, 094901 (2014).
- ³⁵B. H. Tan, R. H. Pelton, and K. C. Tam, "Microstructure and rheological properties of thermo-responsive poly(N-isopropylacrylamide) microgels," *Polymers* **51**, 3238–3243 (2010).
- ³⁶P. W. Zhu and D. H. Napper, "Light scattering studies of poly(N-isopropylacrylamide) microgel particle in mixed water-acetic acid solvents," *Macromol. Chem. Phys.* **200**, 1950–1955 (1999).
- ³⁷T. Suzuki, T. Karino, F. Ikkai, and M. Shibayama, "pH dependence of macroscopic swelling and microscopic structures for thermo/pH-sensitive gels with different charge distributions," *Macromolecules* **41**, 9882–9889 (2008).
- ³⁸K. Kratz and W. Eimer, "Swelling properties of colloidal poly(N-isopropylacrylamide) microgels in solution," *Ber. Bunsenges. Phys. Chem.* **102**, 848–854 (1998).
- ³⁹K. Kratz, T. Hellweg, and W. Eimer, "Structural changes in PNIPAM microgel particles as seen by SANS, DLS and EM techniques," *Polymer* **42**, 6631–6639 (2001).
- ⁴⁰L. Bao and L. Zhaj, "Preparation of poly(N-isopropylacrylamide) microgels using different initiators under various pH values," *Macromol. Sci.* **43**, 1765–1771 (2006).
- ⁴¹T. Hellweg, C. D. Dewhurst, W. Eimer, and K. Kratz, "PNIPAM-copolymer core-shell microgels: Structure, swelling behavior, and crystallization," *Langmuir* **20**, 4333–4335 (2004).
- ⁴²F. Ikkai and M. Shibayama, "Gel-size dependence of temperature-induced microphase separation in weakly-charged polymer gels," *Polymer* **48**, 2387–2394 (2007).
- ⁴³Z. Hu and X. Xia, "Hydrogel nanoparticle dispersions with inverse thermoreversible gelation," *Adv. Mater.* **16**, 305–309 (2004).
- ⁴⁴J. Ma, B. Fan, B. Liang, and J. Xu, "Synthesis and characterization of poly(N-isopropylacrylamide)/Poly(acrylic acid) semi-IPN nanocomposite microgels," *J. Colloid Interface Sci.* **341**, 88–93 (2010).
- ⁴⁵K. Kratz, T. Hellweg, and W. Eimer, "Influence of charge density on the swelling of colloidal poly(N-isopropylacrylamide-co-acrylic acid) microgels," *Colloids Surf., A* **170**, 137–149 (2000).
- ⁴⁶K. Kratz, T. Hellweg, and W. Eimer, "Effect of connectivity and charge density on the swelling and local structure and dynamic properties of colloidal PNIPAM microgels," *Ber. Bunsenges. Phys. Chem.* **102**, 1603–1608 (1998).
- ⁴⁷X. Xia and Z. Hu, "Synthesis and light scattering study of microgels with interpenetrating polymer networks," *Langmuir* **20**, 2094–2098 (2004).
- ⁴⁸C. D. Jones and L. A. Lyon, "Synthesis and characterization of multiresponsive core-shell microgels," *Macromolecules* **33**, 8301–8303 (2000).
- ⁴⁹W. Xiong, X. Gao, Y. Zao, H. Xu, and X. Yang, "The dual temperature/pH-sensitive multiphase behavior of poly(N-isopropylacrylamide-co-acrylic acid) microgels for potential application in *in situ* gelling system," *Colloids Surf., B* **84**, 103–110 (2011).
- ⁵⁰Z. Meng, J. K. Cho, S. Debord, V. Breedveld, and L. A. Lyon, "Crystallization behavior of soft, attractive microgels," *J. Phys. Chem. B* **111**, 6992–6997 (2007).
- ⁵¹L. A. Lyon, J. D. Debord, S. B. Debord, C. D. Jones, J. G. McGrath, and M. J. Serpe, "Microgel colloidal crystals," *J. Phys. Chem. B* **108**, 19099–19108 (2004).
- ⁵²P. Holmqvist, P. S. Mohanty, G. Nägele, P. Schurtenberger, and M. Heinen, "Structure and dynamics of loosely cross-linked ionic microgel dispersions in the fluid regime," *Phys. Rev. Lett.* **109**, 048302 (2012).
- ⁵³S. B. Debord and L. A. Lyon, "Influence of particle volume fraction on packing in responsive hydrogel colloidal crystals," *J. Phys. Chem. B* **107**, 2927–2932 (2003).
- ⁵⁴J. Zhou, G. Wang, L. Zou, L. Tang, M. Marquez, and Z. Hu, "Viscoelastic behavior and *in vivo* release study of microgel dispersions with inverse thermoreversible gelation," *Biomacromolecules* **9**, 142–148 (2008).
- ⁵⁵Z. Xing, C. Wang, J. Yan, L. Zhang, L. Li, and L. Zha, "pH/temperature dual stimuli-responsive microcapsules with interpenetrating polymer network structure," *Colloid Polym. Sci.* **288**, 1723–1729 (2010).
- ⁵⁶X. Liu, H. Guo, and L. Zha, "Study of pH/temperature dual stimuli-responsive nanogels with interpenetrating polymer network structure," *Polym. Int.* **61**, 1144–1150 (2012).
- ⁵⁷J. J. Chen, A. L. Ahmad, and B. S. Ooi, "Poly(N-isopropylacrylamide-co-acrylic acid) hydrogels for copper ion adsorption: Equilibrium isotherms, kinetic and thermodynamic studies," *J. Environ. Chem. Eng.* **1**, 339–348 (2013).
- ⁵⁸X. Xia, Z. Hua, and M. Marquez, "Physically bonded nanoparticle networks: A novel drug delivery system," *J. Controlled Release* **103**, 21–30 (2005).
- ⁵⁹V. Nigro, R. Angelini, M. Bertoldo, V. Castelvetro, G. Ruocco, and B. Ruzicka, "Dynamic light scattering study of temperature and pH sensitive colloidal microgels," *J. Non-Cryst. Solids* **407**, 361–366 (2015).
- ⁶⁰M. Shibayama, T. Tanaka, and C. C. Han, "Small angle neutron scattering study of poly(N-isopropyl acrylamide) gels near their volume-phase transition temperature," *J. Chem. Phys.* **97**, 6829 (1992).
- ⁶¹See supplementary material at <http://dx.doi.org/10.1063/1.4930885> for additional details about the IPN microparticles synthesis.
- ⁶²ISIS-TS2 is the second target station of the ISIS pulsed neutron source operating in the UK. More information is available on the website: <http://www.isis.stfc.ac.uk/>.
- ⁶³B. Sierra-Martin, J. R. Retama, M. Laurenti, A. F. Barbero, and E. L. Cabarcos, "Structure and polymer dynamics within PNIPAM-based microgel particles," *Adv. Colloid Interface Sci.* **205**, 113–123 (2014).
- ⁶⁴M. Shibayama, "Small angle neutron scattering on polymer gels: phase behavior, inhomogeneities and deformation mechanisms," *Polym. J.* **43**, 18–34 (2011).
- ⁶⁵S. Mallam, F. Horkay, A. M. Hecht, A. R. Rennie, and E. Geissler, "Microscopic and macroscopic thermodynamic observations in swollen poly(dimethylsiloxane) networks," *Macromolecules* **24**, 543–548 (1991).
- ⁶⁶M. Shibayama, "Spatial inhomogeneity and dynamic fluctuations of polymer gels," *Macromol. Chem. Phys.* **199**, 1–30 (1998).
- ⁶⁷G. Sudre, D. Hourdet, C. Creton, F. Cousin, and Y. Tran, "Probing pH-responsive interactions between polymer brushed and hydrogels by neutron reflectivity," *Langmuir* **30**, 9700–9706 (2014).